JOURNAL OF PROPULSION AND POWER
Vol. 11, No. 6, November–December 1995

Design Studies of the Advanced Technology Engine

H. F. R. Schöyer*
European Space Agency, 2200 AG Noordwijk, The Netherlands
M. Caporicci†
European Space Agency, 75738 Paris 15, France
and
B. Hufenbach‡ and A.-J. Schnorhk‡
European Space Agency, 2200 AG Noordwijk, The Netherlands

The need was identified for a high-performance bipropellant rocket engine in the 20-kN range for use with Ariane 5, for the transfer of telecommunication satellites to geostationary orbit, and for scientific (interplanetary) missions. The concept deals with a high-performance, pump-fed storable bipropellant engine using monomethyl hydrazine and nitrogen tetroxide propellants. Its target specific impulse of 345 s is close to the theoretical maximum value possible for this propellant combination. The versatility of the advanced technology engine may be enhanced by using it in combination with a general purpose orbital propulsion module for the transfer of stacks of two or three satellites. To develop the concept in detail, design and study contracts were placed with five European propulsion companies. Engine requirements were derived from mission analyses. The studies lead to the selection of a precombustion cycle engine design with a specific impulse over 350 s, which could be developed in Europe in eight years for a cost of 123 million accounting units.

Nomenclature

C^* = characteristic velocity
I_{sp} = specific impulse
p_c = chamber pressure
ε = nozzle expansion ratio, exit area/throat area

I. Introduction

TO assess the usefulness of a high-performance bipropellant engine, for use as an upper-stage engine, an apogee boost motor (ABM), or an engine for interplanetary missions, a number of mission analyses were made. The performance of such an engine was compared with existing engines or engines under development. The mission analyses also served to define engine requirements.

One of the main objectives of the detailed design studies was to investigate whether the high-target specific impulse (≥345 s) was feasible, and whether such a development would be possible within Europe. After various engine cycle studies, a final tradeoff was made between a high-pressure gas generator (HPGG) cycle and a precombustion (PC) cycle. Because of its higher performance, better capacity for future growth, and the wish to stimulate advanced technologies, the PC cycle was selected. For the main components detailed designs were made. Two engine versions emerged: one regeneratively cooled with a metallic chamber and nozzle and the other one film cooled, with a ceramic composite thrust chamber and nozzle. For a similar performance, the ceramic version is about 20 kg lighter. The engine would increase payload mass capabilities for all space missions; in particular, when used as an upper stage for the Ariane 5 launcher; in that case it would increase the Ariane 5 payload capability by 10%.

Based on the detailed designs, development, test, and cost plans were made. They indicate that an engine may be developed in eight years for a cost of 123 million accounting units (MAU) + 17 MAU for a technology phase. The recurring costs of the engine are estimated at 1.68 MAU (all costs at 1990 economic conditions).

II. Mission Analysis and Applications for the ATE

The objective of the mission analysis is on one hand to identify the potential for the ATE from a mission point of view and on the other hand to derive the operational requirements for the engine. The ATE was initially compared with various existing engines, or engines under development, for a number of missions: Earth Orbital Missions, a Comet Rendez-Vous and Return Mission, and a Mars Orbit and Return Mission. Engine performances are given in Table 1 with the launch vehicles: Ariane 5 and Titan 4.

A. Earth Orbital Missions

The detailed mission analysis was made by Smalley[1] with a sophisticated optimization code. This code also analyzed the optimum steering strategy (four were considered). In most cases tangential steering gave optimal results; in a few cases single axis slew steering gave a minor advantage.

Three types of transfer were considered: 1) LEO ⇒ GEO, 2) GTO ⇒ GEO, and 3) LEO ⇒ GTO. (LEO = low Earth orbit, GEO = geostationary orbit, and GTO = geostationary transfer orbit.) Two effects dominate performance: specific impulse and thrust level. If one has low thrust levels, gravity losses become important for trajectories starting from LEO. With two burns, the gravity losses for the ATE are only 2%. For engines with a lower thrust (3 kN), gravity losses easily amount to 17%. These losses may be reduced by increasing the number of burns near the apogee.

The results of mission analyses, for launches with Titan 4 and Ariane 5, based on Hohmann transfers, are given in Table 1. The upper-stage engines that were considered, their main characteristics, the launcher performance, as well as their target orbits, are also listed. In case of delivery to GTO, the

Presented as Paper 92-3662 at the AIAA/SAE/ASME/ASEE 28th Joint Propulsion Conference and Exhibit, Nashville, TN, July 6–8, 1992; received Oct. 4, 1992; revision received Jan. 25, 1995; accepted for publication Feb. 3, 1995.

*Senior Propulsion Engineer for Special Assignments, European Space Research and Technology Centre, P.O. Box 299. Senior Member AIAA.
†Propulsion Engineer, ESA Headquarters, 8-10 Rue Mario Nikis.
‡Propulsion Engineer, European Space Research and Technology Centre, P.O. Box 299. Member AIAA.

Table 1 Launcher characteristics, engine performance, and payload into orbit

Launcher				Ariane 5		Titan 4	
Apogee × perigee, target orbit				550 × 550 km		259 × 148 km	
Inclination, target orbit				7 deg		28.6 deg	
Payload into target orbit, kg				18,000		17,800	
Engine	Thrust, kN	I_{sp}, m/s	Remarks	LEO–GEO, kg	LEO–GTO, kg	LEO–GEO, kg	LEO–GTO, kg
L-7	27.5	3099	Pressure fed	5242	8416	4475	8104
Transtage	17	3217	Pump fed	5485	8653	4706	8339
XLR 132	16.7	3334	Pump fed	5719	8879	4933	8565
ATE	20	3383	Pump fed	5814	8971	5025	8657
STAR-75	202	2824	Solid motor	—	7316[a]	—	7010[a]

[a]2 × STAR-75.

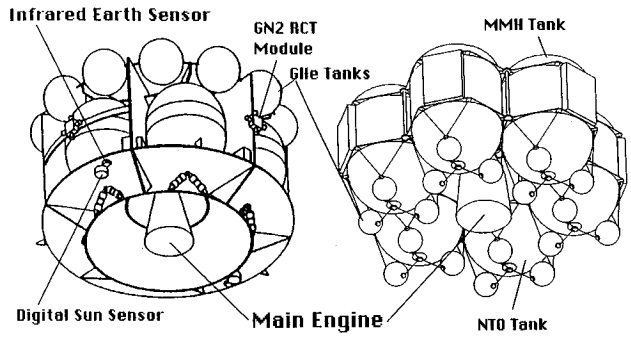

Fig. 1 OPMs for the ATE; left: dedicated OPM,[2] right: modular OPM.[3]

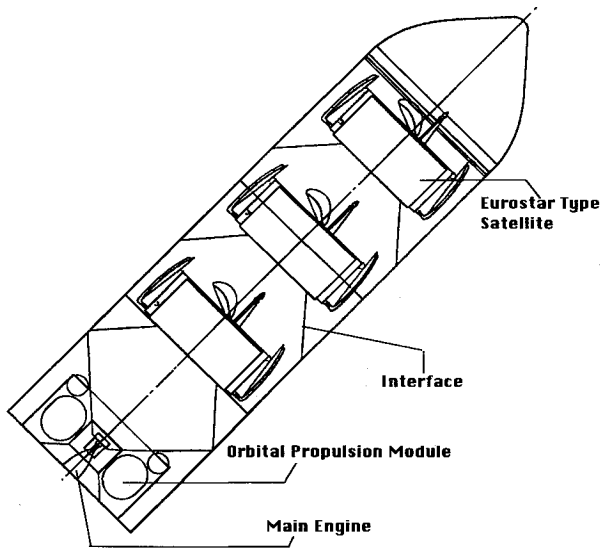

Fig. 2 Stacking of satellites on an OPM for an Ariane 5 configuration.

satellite ABM has to inject the satellite into GEO. In case of delivery to GEO, no satellite ABM is required.

Due to its high target I_{sp} (3383 m/s), the ATE in all cases injects the highest mass in orbit. Pressure-fed systems are penalized by their high tank mass because of high tank pressures. Titan 4 suffers from the high inclination of its launch site as compared to Ariane 5. In all cases the GEO target orbit had a 0-deg inclination. As all engines have a high thrust level, gravity losses are comparable and small. The mission analyses identified that for ATE Earth orbital missions, the longest total burn time is 34 min.

B. Orbital Propulsion Module and Stacking

The ATE takes full advantage of Titan's and Ariane 5's capacity to launch two or more spacecraft simultaneously. By using an orbital propulsion module (OPM) it is possible to transfer each satellite directly from LEO (or GTO) into its required GEO position, eliminating the need for a separate ABM for each satellite. The OPM is a fully autonomous stage, with its own control system. The ATE allows for thrust vector control (TVC), whereas cold-gas thrusters are used for roll-control and small attitude corrections. Two designs were made for OPMs. Kruzins[2] reported on a dedicated OPM, whereas Hobbs[3,4] reported on a modular OPM (Fig. 1). The modules allow the construction of OPMs of various sizes, out of common building blocks.

The OPM carries a stack of satellites, and is housed in the payload bay of the launcher (Fig. 2). After injection into LEO or GTO, the OPM is released and moves to the position where the first (top) satellite is injected. Subsequently, the OPM moves to the next position, releases the next satellite, etc. This eliminates the need for apogee propulsion on individual satellites. After injection of the last satellite, the OPM is put into a graveyard orbit. Of course, the ATE may also be used as a classical ABM for large satellites.

Table 2 Return mission Churyumov–Gerasimenko

	Final mass, kg	Burn time, min	Number of burns
With Ariane 5 (initial mass 15,000 kg)			
Earth escape	4145.5	30.65	3
Retargeting towards Earth	3307.4	2.37	1
Comet arrival maneuver	2438.2	2.47	1
Comet departure maneuver	1877.4	1.59	1
Sum total	—	37.08	6
With Shuttle (initial mass 27,210 kg)			
Earth escape	7480.9	55.68	6
Retargeting towards Earth	5990.8	4.2	1
Comet arrival maneuver	4400.4	4.52	1
Comet departure maneuver	3390.9	2.86	1
Sum total	—	67.26	9

Table 3 Mars return mission

	Final mass, kg	Burn time, min	Number of burns
GTO-heliocentric orbit	5652	6.63	1
Mars arrival maneuver	3042.9	7.37	1
Mars departure maneuver	1640.4	3.96	1
Sum total	—	17.96	3

C. Interplanetary Missions

Two interplanetary missions were analyzed by Elliott[5]: 1) a Comet Rendez-Vous and Return Mission and 2) a Mars-Orbit and Return Mission. Launch vehicles were Ariane 5 (an earlier version with 15,000-kg payload into LEO) or the

U.S. Space Shuttle. For all return missions aerocapture at Earth was assumed.

1. Churyumov–Gerasimenko Mission

For the comet mission, comet Churyumov–Gerasimenko was selected. The results of the mission analysis are presented in Table 2. A similar analysis using a 3-kN engine returned 1560- and 2683-kg mass-to-Earth for Ariane and Shuttle, respectively. This indicates benefits of 300–700 kg, respectively. The useful payload mass for the ATE version is larger by at least 200 kg as the pump-fed ATE allows lighter propellant tanks.

2. Mars Return Mission

This mission was only analyzed using an Ariane 5 with an H-10 cryogenic upper-stage. This configuration puts 8000 kg into GTO, but is not considered for Ariane 5 anymore. The results are given in Table 3. A similar mission with a 3-kN engine would return 1505 kg to Earth.

III. Derived Requirements

The mission analysis is based on the assumption that a specific impulse $I_{sp} > 3383$ m/s can be achieved. The first requirement, therefore, is that this target I_{sp} can be met or exceeded.

For Earth Orbital missions, the longest identified total burn time is 34 min; for interplanetary missions the longest burn time is 67 min on the Shuttle; for an Ariane 5 Comet Return Mission the longest burn time is 37 min. A nominal life of 1 h has been specified. This gives a large margin for all Ariane 5 missions, and is close to what is required for a Shuttle Comet Return Mission. For qualification, 4 h total burn time is required.

The maximum number of burns that has been identified is nine. The ATE is requested to have at least the capability for 10 starts during operation, and 20 starts for qualification. This mainly affects the fatigue life of the thrust chamber if manufactured with coolant slots in a metallic liner.

The thrust level is 20 kN. A higher thrust level would be acceptable and is advantageous for the turbopump design.

No need for throttling could be identified. However, a throttling capability from 90 to 100% full thrust is specified for flexibility. This puts a lower limit on the coolant pressure because the coolant has to remain at supercritical pressures.

TVC is required during orbit transfer and maneuvering. The TVC specifications are 15 deg/s with a maximum deflection of 15 deg in all directions.

For the transient operations, i.e., startup, shutdown, and throttling, the mission analysis does not give clear requirements. For the time being, it is specified that all transient operations shall be accomplished within 3 s.

IV. Cycle Selection

From tradeoff studies[6–8] on a large number of engine cycles, a HPGG cycle (Fig. 3a) and a PC cycle (Figs. 3b and 3c) emerged as the most promising.

All major European liquid propulsion industries participated in selecting the cycle for the ATE. A number of important points emerged, which are summarized in Table 4. The selection is based on an overall assessment of these considerations. There is a slight preference for the PC cycle based on overall performance. The final decision favored the PC cycle. This was also based on the agency's wish to develop advanced technology within Europe. The application of the PC cycle to storable propellants is new for Europe.

V. Engine Design

A. Combustion Chamber Design

A core mixture ratio of 2.32 has been selected to achieve maximum specific impulse. To meet the required thrust of 20 kN a mass flow rate of 5.81 kg/s is required. A chamber pressure of 9 MPa was selected to keep the coolant pressure above the critical pressure.

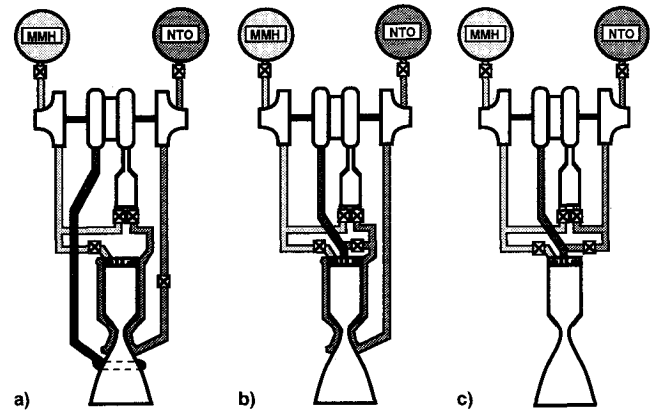

Fig. 3 Engine cycles: a) HPGG cycle, b) PC cycle for metallic version regeneratively cooled, and c) PC cycle for CMC version film-cooled.

The heat flux increases with chamber pressure to the power 0.8. At a chamber pressure of 9 MPa, at most 20% of the fuel is required for film cooling. Detailed heat transfer analyses revealed that the wall temperature limits may be met without film cooling increasing the C^* efficiency from 98 to 99.5% (I_{sp} losses due to film cooling ~70 m/s). Heat transfer analyses indicated that with film cooling it might be possible to increase the chamber pressure to 11 MPa.

An injector pressure drop of 1.5 MPa has been selected, based on experience from the engine manufacturers. However, for the specific types of injectors (see Sec. V.B) the experience is very limited. As a large part of the propellants is injected in gaseous form, no pressure drop for atomization is required. On the other hand, there must be a large enough pressure drop to prevent the chamber pressure variations from disturbing the injection process. Whether the value of 1.5 MPa is sufficient for stable and efficient engine operation must be verified during injector development and engine tests.

Two different designs have been studied: 1) a traditional metallic chamber and 2) a ceramic chamber. The ceramic design saves mass (10 kg) and eliminates the complex regenerative cooling system. Film cooling, in fact, is sufficient to keep the wall temperature below the limit for modern ceramic materials and can maintain the expected high-performance level ($I_{sp} > 3383$ m/s).

1. Metallic Combustion Chamber

The ATE metallic combustion chamber (Fig. 4) is regeneratively cooled by supercritical nitrogen tetroxide (NTO) flowing through 122 longitudinal slots.

The operating chamber pressure is 9 MPa and the overall mixture ratio is 1.86. A 20% fuel film cooling is assumed, but probably is not required. Because of the engine restartability requirements, material fatigue characteristics are important. After an initial tradeoff of various materials, two were assessed in more detail: 1) the copper-based alloy NARloy-Z and 2) the oxide-dispersion strengthened nickel-chromium alloy INCONEL MA754.

NARloy-Z has a high thermal conductivity yielding a low operating temperature (~770 K). It creep-hardens, which reduces bulging of the thin inner walls (creep ratcheting). However, the NTO, used for cooling, requires the cooling channels to be gold coated. Manufacturing of such chambers is well established.

INCONEL MA754, has good high-temperature strength, creep and corrosion resistance, and is compatible with NTO. The operating temperatures are higher than for NARloy-Z (~1300 K). Manufacturing of a superalloy chamber is not yet fully developed. Finite element models of two designs and a

Table 4 Cycle selection criteria

	PC	HPGG
Precombustor	Oxidizer-rich precombustor, two-stage injection[9] required	Fuel-rich gas generator, possible problem of soot deposits in the turbine and high temperatures
Turbopump	Sealing and testing are critical	Aerodynamically loaded partial admission turbine, simple testing, axial balancing, and soot deposits
Turbopump development, costs, and design	Development, costs, and risks higher	Turbopump design is more critical
Main injector	Pintle or swirler injector, development longer and more expensive	Impinging jet injector, recurring costs of the injectors larger
Nozzle extension	Simple nozzle design	Injection of turbine exhaust gases into the nozzle extension is necessary (performance)
System analysis/performance and layout	40–80 m/s more I_{sp}	Difficult to modify in case of future growth
Risk assessment and manufacturing aspects	Better off-design performance, in case of change from PC to HPGG, several PC components can be used without major modifications	Sensitive to individual efficiencies of components; testing and integration is straightforward
Development plan and cost estimate	Development time eight years, development costs 100%. More complex	Development times eight years, development costs 90%
Revenue and market aspects	ΔI_{sp} = 40–80 m/s; this gives 60–120 kg more useful payload into orbit	Less financial benefits for the satellite operator
Conclusion	Preference for PC cycle	——

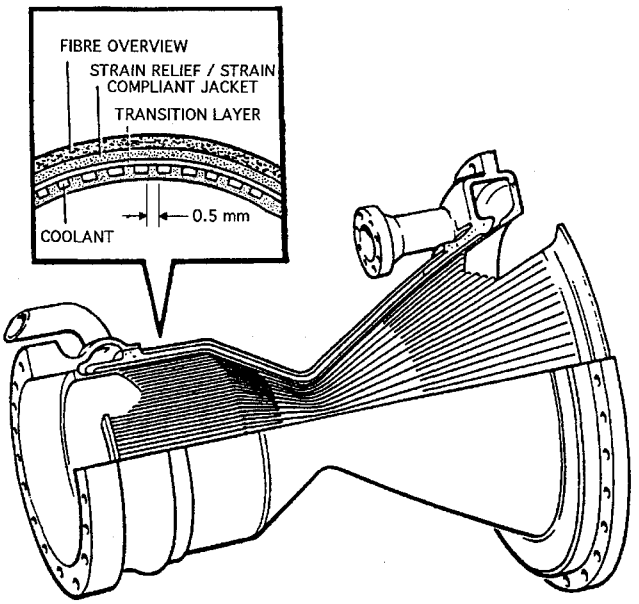

Fig. 4 ATE metallic combustion chamber.

simplified NASA life prediction technique have been used to simulate cyclic loading of the liner[10] and to predict low-cycle fatigue behavior for both materials. Moreover, validation tests were carried out on coupons. The simulation of the cyclic loading indicated that fatigue life for INCONEL MA754 at these high temperatures might not meet the qualification requirements of 20 starts.

NARloy-Z was selected because of its thermal conductivity, its good resistance for cycle fatigue, and because of the doubts with regard to the fatigue life of INCONEL MA754.

The closeout of the coolant channels is by a gold-plated electrodeposited copper transition layer. This is covered by a strain relief compliant jacket that allows thermal expansion and contraction of the inner liner, hence, further reducing the danger of creep ratcheting. The strength of the combustion chamber finally comes from a fiber overview.

2. Ceramic Combustion Chamber

A ceramic composite material design has also been made.[11,12] Two silicon–carbide fiber matrix composites have been considered: 1) SEPCARBINOX 2D (with woven carbon fiber reinforcement) and 2) CERASEP[13] (with woven silicon–carbide reinforcement). Only film cooling and radiation cooling are necessary, since the ceramic materials can withstand working temperatures up to 1870 K. The design is a cylindrical thrust chamber with small contraction ratio; the dimensions are given in Table 5. It is seen here that the contraction ratio and exit area ratio are different for the metallic and ceramic combustion chamber. The smaller contraction ratio for the ceramic combustion chamber stems from manufacturing considerations. The larger exit area ratio for the metallic chamber is because the high wall temperatures require active (regenerative) cooling. As the ceramic material can withstand much higher temperatures, the exit area ratio could be reduced, which is advantageous for the manufacturing process, if a ceramic nozzle is also used.

Table 5 Comparison between CMC and metallic combustion chamber

	CERASEP chamber	Metallic chamber
Chamber length	224 mm	178 mm
Contraction ratio	3	10
Exit area ratio	10	35
Regeneratively cooled	No	Yes
Film cooled	Yes	Possible
Percent fuel used for film cooling	24.3	20
Film mixture ratio, O/F	0.4	0
Film cooling performance losses	72.5 m/s	111.8 m/s
Pressure	9 MPa	9 MPa
Core flow mixture ratio	2.15	2.32
Combustion efficiency	99.5%	99.5%
Overall chamber mass	4 kg	14.1 kg

Maximum mechanical loads and thermal stresses occur immediately after the ignition and determine the dimensions. A wall thickness of 6 mm is required for CERASEP, whereas 4 mm is sufficient for SEPCARBINOX, which has a better thermomechanical behavior but is less oxidation resistant. It can operate in an oxidizing environment for 1 h at maximum. As further mechanical improvement of CERASEP is expected, this material has been selected.

A screwed-bonded coupling joint located at an area ratio of 10 is used to connect the combustion chamber to the nozzle extension. Leak tightness is ensured by a ceramic adhesive seal. The injector can either be brazed to the combustion

Table 6 Results of heat transfer analyses

	Fiat[15]	Volvo[14]
Channel height, mm	2.4	2.4
Heat transfer coefficient, kW/m²/K	28.5	30
Heat flux, MW/m²	74	80
Coolant velocity, m/s	30	45
Gas side wall temperature, K	820	780
Coolant pressure, MPa	14.5	14
Mean coolant specific heat, kJ/kgK	2.98	2.19
Coolant pressure drop, MPa	0.16	0.54
Coolant temperature rise, K	164	254
Coolant enthalpy rise, kJ/kg	488	556
Overall heat transfer, MW	2.0	2.27

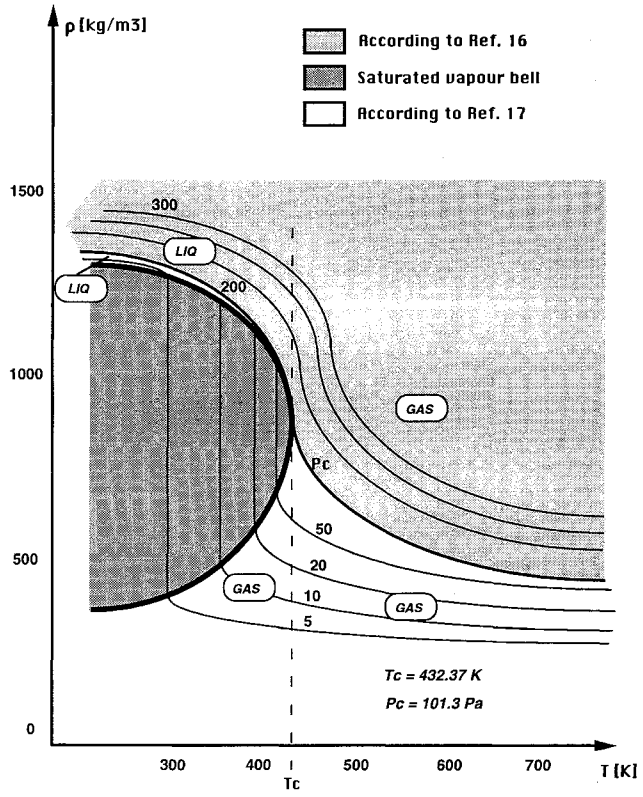

Fig. 5 State diagram for NTO (Ref. 17).

chamber or an expanded graphite seal can be used. These solutions have not yet been demonstrated for the pressure level (9 MPa), but are considered to be feasible in the near future.

3. Regenerative Coolant Analysis

The metallic thrust chamber is regeneratively cooled with supercritical NTO. The high heat fluxes exclude the use of monomethyl hydrazine (MMH) (decomposition). The cooling system has to meet the following requirements: the minimum coolant static pressure at the throat section has to be well above the critical pressure of NTO (10.1 MPa) to avoid nucleate or film boiling (this implies a minimum channel height ≥1 mm) and the maximum wall temperature (for NARloy-Z) has to be well below 820 K. The results of different coolant analyses[14,15] are summarized in Table 6.

The results mainly differ with regard to the coolant channel pressure loss and the wall temperature distribution. This difference is rather small considering the uncertainty in convective heat transfer calculations. Where lower wall temperatures were calculated[14] this was due to an enhancement of the coolant heat transfer coefficient because of NTO dissociation, a different approach to calculate the friction factor, and subsequent higher coolant pressure drops. These differences also lead to different values for the mean specific heat of the coolant.

Regenerative cooling seems feasible without additional film cooling. However, in case it would not be sufficient, film cooling is possible. The maximum heat flux in the throat region is below 80 MW/m² (for comparison: maximum heat flux of SSME 120 MW/m²). However, there is a lack of experimental data concerning the quantitative effect of NTO dissociation on the wall-to-coolant heat transfer, and the accuracy of the calculated thermodynamic properties of supercritical NTO is limited by the state of the art of the theory. Only experimental work can improve this situation.

4. Thermodynamic and Transport Properties of NTO

The thermodynamic and transport properties of NTO under supercritical conditions have been investigated.[16] The NTO working domain (Fig. 5) has been divided into two parts: 1) the "liquid domain" for temperatures lower than the critical one and 2) the "gaseous domain" for higher temperatures.

In the gaseous domain, as NTO decomposes ($N_2O_4 \Leftrightarrow 2NO_2$), chemical equilibrium is calculated by minimizing the Gibbs free energy. The volumetric behavior is described by the Redlich–Kwong equation of state. Thermodynamic properties are computed for an ideal gas and then corrected for pressure effects. The heat of reaction (of NTO decomposition) is taken into account for heat capacity and thermal conductivity. The transport properties (viscosity and thermal conductivity) have been determined by the Chapman–Enskog theory. In the liquid domain, no dissociation is assumed. The volumetric behavior of NTO has been calculated by using the corresponding state liquid correlation (COSTALD), developed by Hankinson and Thompson and extended by Brobst to the compressed liquid zone. The thermodynamic and transport properties are based on experimental results from the literature.

The results obtained are physically meaningful except in the region close to the critical point. This is due to the lack of theoretical models and experimental results describing this region. However, the overall result is not affected.

5. Film Cooling Analysis

For the ceramic matrix composite CMC (CERASEP) combustion chamber, the regenerative cooling is replaced by film cooling. This simplifies the cycle layout as shown in Fig. 3c. Using in-house computer codes, the film cooling was optimized, taking into account the engine requirements and the material limitations (1870 K). A gaseous film with an initial mixture ratio of 0.4 and an MMH mass flow rate equal to 24.3% of the total MMH flow rate has been selected. The film cooling mixture ratio and the temperature evolution along the chamber are given in Fig. 6. The film cooling efficiency was estimated to 98% (I_{sp} losses).

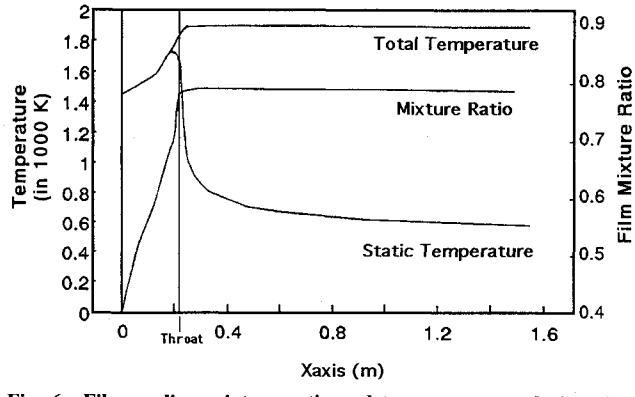

Fig. 6 Film cooling mixture ratio and temperature evolution along the chamber profile.[11,12]

B. Injector Design

The ATE injector must produce stable and efficient combustion between 100–90% nominal thrust, during startup and shutdown transients. In the proposed precombustion cycle the injector uses three streams of fluid. The hot oxidizer (380 K) coming from the regenerative cooling circuit is mixed with oxidizer-rich hot gases from the turbine (830 K). This mixture is introduced into the combustion chamber either via a central pintle-type injector (Fig. 7a) or through a swirler (Fig. 7b).

Fuel is admitted to the chamber via multiple orifices surrounding the pintle or the swirler. Part of the fuel may be directed towards the chamber wall to provide film cooling if necessary. The injector may have acoustic cavities along its periphery to enhance combustion stability. Since the oxidizer is at high temperature when it enters the injector and mixes with a roughly equal mass flow rate of very hot turbine exhaust gases, heat transfer to the fuel might cause premature decomposition of the MMH and there is also a high risk of thermal damage to the pintle. Therefore, a thermal barrier has been placed in the injector body (Fig. 7). Protection of the pintle may be by cooling it with oxidizer coolant (380 K); alternatively, a refractory metal may be used for the pintle. The use of three fluid streams requires an extensive test program to achieve high combustion efficiency and stability under operational conditions.

For the ceramic version a classical impingement or coaxial injector is foreseen. The NTO and the precombustor gases are mixed before passing through the injector. As there is no coolant pressure drop, an injector pressure drop up to 2 MPa is available and is considered to be sufficient.

C. Precombustor Design

An axial flow precombustor[9] with secondary injection and an oxidizer-rich mixture ratio has been selected because the decomposition temperature of MMH for a fuel-rich mixture exceeds the maximum inlet temperature for metallic turbines (1079 K) by more than 100 K. It has the advantage of a simple design. The hot flow can easily be confined to the center to prevent wall burnout problems, which are typical for the more complex reverse flow-type precombustors. Although an oxidizer-rich mixture ratio leads to a corrosive environment while the specific propellant consumption is higher, this type of precombustor was selected. In addition, the Russian experience with oxidizer-rich combustors confirms this concept, although this was not known at the time of the design. The high overall precombustor mixture ratio ($\geq$15) requires secondary oxidizer injection for two reasons: first, to ensure stable and efficient combustion in a primary mixing and combustion zone (close to stoichiometric mixture ratios) and second to enhance turbulence in order to prevent hot spots (stratified flow) that might damage the precombustor and the turbine blades. The primary mixing and combustion zone is surrounded by a double-walled cylinder. The secondary oxidizer flow provides cooling of the primary mixing and combustion zone by flowing through this double-walled cylinder before it is injected into the precombustor.

A preliminary sizing of the precombustor resulted in a length $\leq$250 mm and a diameter ~50 mm. This size fits well in the overall envelope of the ATE. CRES347 was selected, because of its corrosion resistance. The maximum encountered wall temperature is well below 550 K. The mass of the precombustor including injector is estimated as 1.5 kg.

The resulting low C^* value (694 m/s) is due to the oxidizer rich mixture ratio. It is based on experiments with NTO and hydrazine in the oxidizer-rich region.[18] However, the precombustor efficiency hardly affects the overall engine efficiency.

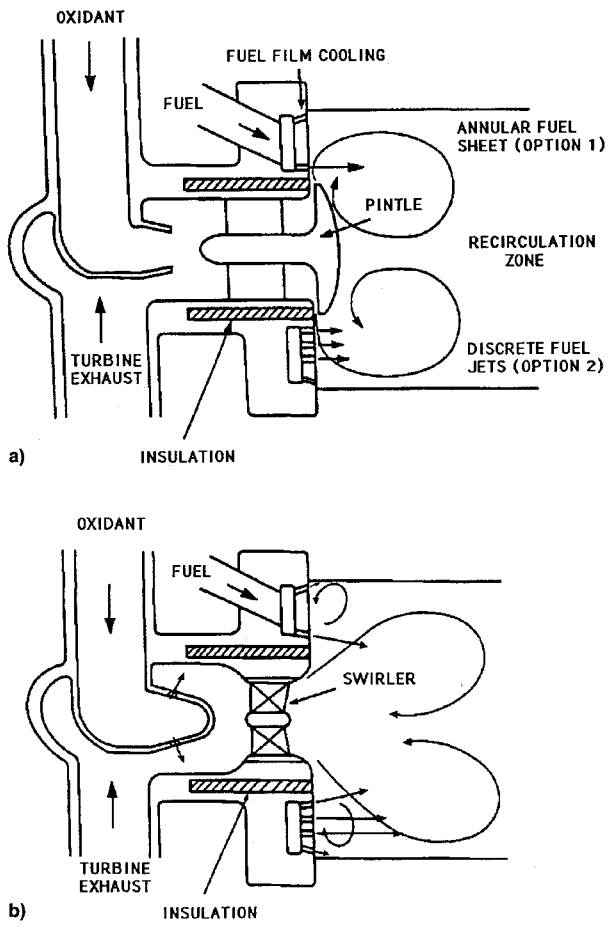

Fig. 7 Injector designs.

D. Turbopump

Several designs have been made and analyzed. All have a single shaft arrangement with oxidizer and fuel centrifugal shrouded pumps positioned at each shaft end (Fig. 8). The shaft is driven by a single-stage axial flow turbine located between the pumps because of cavitation and shaft critical speed. The main turbopump parameters are listed in Table 7.

The turbopump rotational speed has been optimized with regard to the NTO pump delivery pressure considering speed limitations due to minimum machinable turbine blade dimensions and pump impeller size, a maximum turbine blade stress factor, and a maximum bearing speed.

A turbine entry temperature of 779 K was selected to keep the turbine expansion ratio low and to avoid excessive pump delivery pressures; this leaves sufficient margin with respect to the maximum turbine blade temperature of 1079 K. For the precombustion cycle the effect of turbopump efficiency on I_{sp} is marginal.

The oxidizer pump is equipped with an inducer to avoid cavitation. The shaft is rotating below the first critical speed. Due to the high pressure and rotational speed, the bearing

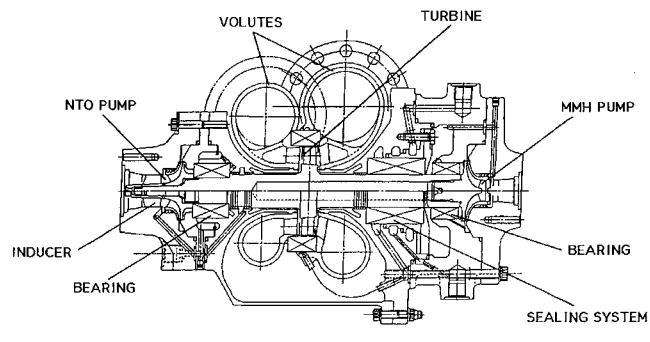

Fig. 8 Turbopump design.

Table 7 Turbopump performance

	Fiat		Volvo		SEP		Royal Ordnance	
Rotational speed, rpm	76,394		60,000		76,394		76,394	
TURBINE type	Reaction, single stage		Reaction, single stage, 50% admission		Reaction, single stage, ceramic		Reaction, single stage	
Inlet pressure, MPa	12.66		14.7		14.5		14.5	
Outlet pressure, MPa	10.94		12.5		13.5		10.5	
Inlet temperature, K	800		990		1300		779	
Mass flow rate, kg/s	4.209		4.41		1.8		3.16	
T-T expansion ratio	1.15		1.23		1.075		1.38	
T-T efficiency	0.808		0.83		—		0.9	
Shaft power, kW	116.5		176		145		162	
PUMP type	NTO[a]	MMH[b]	NTO[a]	MMH[b]	NTO[a]	MMH[a]	NTO[a]	MMH[b]
Inlet pressure, MPa	0.4	0.4	0.4	0.4	0.4	0.4	0.4	0.4
Delivery pressure, MPa	15.2	12.6	20.8	18.8	17	17	19.5	18.1
Mass flow rate, kg/s	4.088	1.762	4.01	1.83	3.74	2.17	3.77	2.03
Specific speed	0.419	0.279	0.26	0.16	0.348	0.223	0.330	0.227
Efficiency	0.59	0.537	0.59	0.54	0.64	0.57	0.59	0.54
Required power, kW	70.7	45.8	98.3	72.7	65	80	85	76
Inlet outer diameter, mm	20	14	21	15	18	—	—	—
Impeller outer diameter, mm	36	41	54	57	36	45	—	—
Impeller exit height, mm	1.1	0.7	1.5	1.5	1.5	1.7	—	—

[a]1 axial + 1 centrifugal. [b]1 centrifugal.

and seal designs are critical. Seals are purged with helium while bearings are cooled and lubricated by the propellants.

The turbopump designs have very high rotational speeds. It is nevertheless possible to operate below the first critical speed due to the small dimensions of the rotating parts, the turbopump layout that leads to a good mass distribution and an adequate location of the bearings, and because of the proper selection of stiff bearings.

The turbine is started by helium supply until 24,000 rpm is reached. Then hot gases are supplied by the precombustor.

The possibility of using CMC for the turbine wheel and the shaft was also investigated. This turned out not to be an option (see Sec. VI.B) because of the limited advantage compared to the metallic option.

E. Nozzle Extension

As was done for the combustion chamber, two options were studied for the nozzle: 1) a metallic and 2) a ceramic version.

1. Metallic Nozzle Extension

A detailed investigation[19] of the various losses in the nozzle extension showed a slightly lower nozzle efficiency than originally estimated. The boundary-layer losses, kinetic losses, and divergence losses add up to 5.3%. Additionally, 2% I_{sp} losses were considered in case of film cooling. Heat losses due to regenerative cooling and low outer wall temperatures are negligible.

The nozzle shape was determined by the Rao method.[20] Design parameters and fundamental results are shown in Table 8.

The divergence losses were estimated by comparing the ideal one-dimensional I_{sp} with that given by two-dimensional calculations. An efficiency of 0.991 was derived. Kinetic losses were determined by the RCTP (Ref. 21) computer code (JANNAF procedure) and boundary-layer losses were computed by the STAN5 code (Spalding–Patankar theory). Following this, the wall temperatures and heat transfer coefficients were calculated accounting for insulation and cooling. As a result of stress analyses by two-dimensional finite element methods (FEMs), the thickness immediately downstream of the flange where maximum temperature occurs was increased to achieve a long creep life.

2. Ceramic Nozzle Extension

Also, a ceramic extension design was made[11] based on SEPCARBINOX–Novoltex material. This is a C-SiC matrix reinforced by a carbon-based Novoltex texture. Experience exists with manufacturing and firing of an HM7 engine with a Novoltex ceramic nozzle. The oxidation resistance of this composite still has to be validated for long firing times. The design is based on a parabolic contour. The main difference to a steel nozzle extension is the maximum adiabatic wall temperature of 1870 K.

Table 8 Nozzle design parameters and results for p_c = 9 MPa; expansion ratio, ϵ = 400

Parameter	Value
Length, mm	910
Length injector exit, mm	1506
Throat radius, mm	19
Nozzle exit radius, mm	380
Nozzle exit angle, deg	10
Wall thickness, mm	3.0
Material	Steel
Mass, kg	20

Table 9 Comparison between CMC and metallic nozzle extension

	SEPCARBINOX nozzle	Metallic nozzle
Length throat-exit, mm	1324	1329
Bell type	Parabolic	Rao
Starting area ratio	10	35
Maximum wall temperature, K	1800	850
Nozzle efficiency, %	97.7	97.7
Nozzle mass, kg	14	20

For a ceramic combustion chamber and nozzle the gimballing actuators have to be mounted on the injection plate. If both combustion chamber and nozzle extension are made from composite material a screwed-bonded coupling can be used. If a metallic combustion chamber is adopted, this has a bolted flange joint at an area ratio of 35; an expanded graphite seal ensures leak tightness.

The use of SEPCARBINOX–Novoltex for the nozzle extension provides substantial weight savings (6 kg). Production is possible without major developments and its cost is comparable to that of the metallic nozzle. A comparison between a ceramic nozzle and a metallic one is given in Table 9.

F. Control System

The engine control system is required to set and maintain the engine operation conditions within a specified margin of accuracy and stability. The control system has to provide a reliable start and shutdown sequence with a transient time ≤3 s, stable operation, and health monitoring of the engine.

The fast transients during startup and shutdown of the engine were modeled and analyzed in detail. Various safe and reliable sequences have been defined. In any case the calculated transient times[22] (1.1 s for startup, 2.15 s for shutdown, and 0.5 s for throttling from 100 to 90% thrust) easily meet the requirements.

In order to define the number and location of flow control valves that are required for throttling, the steady-state off-design performance of the engine was analyzed again. Stable off-design engine operation at constant turbopump rotational speed and turbine inlet temperature can be provided using four flow control valves of which two are located in the main chamber lines and two in the precombustor lines of the oxidizer and fuel. To reduce the complexity of the control concepts, concepts based on three- and two-flow control valves were investigated. Stable operation is possible using only two valves, allowing a reduction in turbopump rotational speed and turbine inlet temperature. Figure 9 summarizes the results for the two-valve concept. Both valves are located in the precombustor lines.

Also shown in Fig. 9 are two latching valves located upstream of the pumps for starting and shutdown of the engine. Pressure and temperature sensors at main engine locations as well as a turbopump rotational speed sensor are required for monitoring the engine operation.

VI. Performance Estimate

A. Metallic Version

The precombustion cycle has been optimized[23–26] using the cycle analysis code "CATE." The results are summarized in Table 10. The design and performance of various components have also independently been verified in detail.

The important conclusion is, that indeed, a storable bipropellant engine with an $I_{sp} \geq 345$ s (3384.5 m/s) is feasible.

B. Ceramic Version

The main changes are the deletion of the regenerative cooling that results in a lower oxidizer pump delivery pressure, change to a classical impinging or coaxial injector, and film cooling. Furthermore, the optimum chamber pressure has to be established, since NTO does not have to be above the critical pressure.

A ceramic precombustor and turbine were also considered: the precombustor mixture ratio becomes fuel-rich due to the incompatibility of CMCs with the corrosive environment of an oxidizer-rich mixture. As a result the turbine inlet temperature increases from 779 to 1300 K.

The advantage is a decrease of the turbine expansion ratio, resulting in lower pressures. The small expansion ratio together with small mass flow rates leads to very large turbine

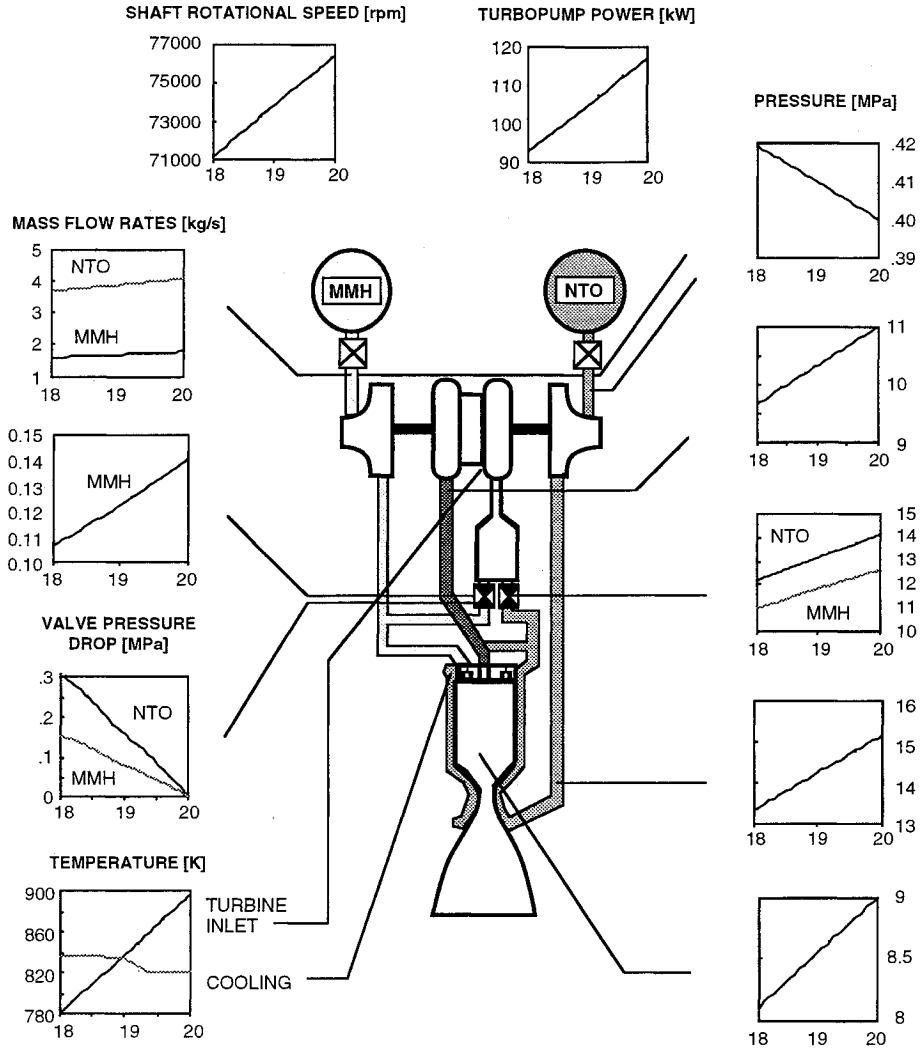

Fig. 9 Cycle pressures (MPa), mass flow rates (kg/s) and component characteristics vs engine thrust (kN) for a two-valve arrangement.

Table 10 Main component performance

	Unit value
Main combustion chamber	
Core mixture ratio	2.32
Overall mixture ratio	1.86
Chamber pressure, MPa	9.0
Injector pressure drop, MPa	1.5
Overall mass flow rate, kg/s	5.81
Characteristic velocity, m/s	1,705
C^* efficiency, %	98
Nozzle extension	
Thrust coefficient	2.02
Thrust coefficient efficiency, %	97
Vacuum thrust, kN	20
Vacuum specific impulse, m/s	3,446.1
Precombustor	
Precombustion pressure, MPa	14.5
Primary mixture ratio	3
Overall mixture ratio	15
Injector pressure drop, MPa	2.9
Mass flow rate, kg/s	3.218
Characteristic velocity, m/s	694
C^* efficiency, %	67.3
Turbine	
Inlet temperature, K	779
Expansion ratio	1.38
Efficiency (T-S), %	87
Rotational speed, rpm	76,394
Shaft power, kW	162
Tank conditions	
Temperature, K	298
Pressure, MPa	0.5
Oxidizer pump	
Inlet pressure, MPa	0.4
Outlet pressure, MPa	19.5
Power, kW	85
Mass flow rate, kg/s	3.77
Efficiency, %	59
Fuel pump	
Inlet pressure, MPa	0.4
Outlet pressure, MPa	18.1
Power, kW	76
Mass flow rate, kg/s	2.03
Efficiency, %	54

blade height-to-diameter ratios, resulting in a low efficiency and in high structural loads. Therefore, the use of ceramics for the precombustor and the turbine is not of interest.

C. Mass Breakdown

Table 11 shows the mass breakdown for the metallic and ceramic versions. Application of ceramics reduces engine mass by 22%. The main savings are for the combustion chamber (10 kg) and nozzle (6 kg).

VII. Development/Cost Plan

The overall development plan is a compromise between minimizing resources (cost and time) and development risk.

The development is complemented by a technology phase of 17 MAU, lasting three years, (for new technologies) and running in parallel with the breadboard phase. The three

Table 11 Mass breakdown of metallic and ceramic version

	Metallic, kg	Ceramic, kg
Precombustor	1.3	1.3
Main injector	5.2	5.0
Combustion chamber	14.1	4.0
Nozzle extension	20.0	14.0
Valves	14.0	14.0
Flanges and pipe work	4.1	4.1
Turbopump	15.5	15.5
Σ	74.2	57.9

Table 12 Required hardware for development testing

Phase	Bread-board	Devel-opment	Quali-fication	Σ
Engines	2	4	1	7
Turbopumps	5	4	1	11
Nozzle extensions	3	4	1	8
Precombustors	4	4	1	9
Combustion chambers	4	5	1	10
Gimbals	—	2	1	3

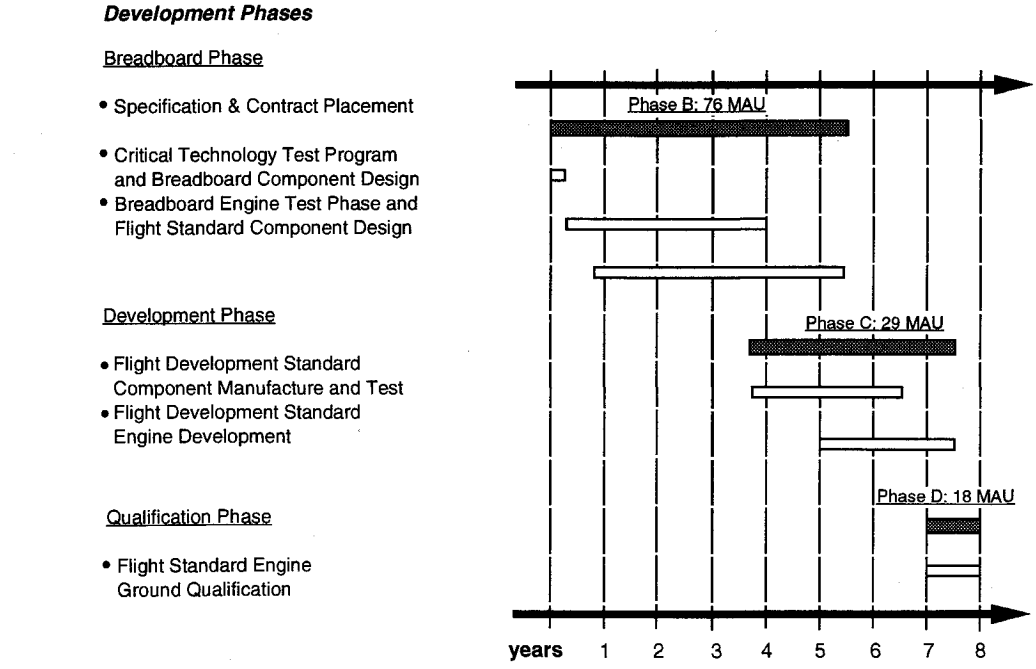

Fig. 10 Development time schedule.

major phases: 1) breadboard, 2) development, and 3) qualification and their subphases are shown in Fig. 10. In the breadboard phase the basic component and engine performance is verified and optimized. All major design iterations take place in this phase. Tests at engine level are performed as early as possible.

During the development phase it is verified that the engine meets its specification. The development configuration includes all improved design features of the breadboard phase. The performance will be tested throughout the whole operational envelope. During the qualification phase the engine as well as the manufacturing processes will be ground-qualified. The qualification model is identical to the last development model.

Figure 10 also shows the nominal time scale and costs. Together with the development time scales and costs, the risks were also estimated. The nominal time scale assumes that no major problems will be encountered. Including all contingencies due to risks, the development would take 12 years. While the nominal development cost amounts to 123 MAU spread over eight years; the development cost, inclusive all contingencies, would amount to 297.5 MAU. The development time may be reduced by using duplicate test facilities and parallel development efforts; this, however, would increase the development costs.

The engine has a nominal mission life of 1 h and is 10 times restartable. The operational life is 2 h and the engine will be qualified for 4 h and 20 cycles. The number of engines (7) and components for testing in each phase are given in Table 12.

VIII. Testing

For a precombustion cycle engine extensive and integrated testing is necessary. Not only testing of the individual components, but also of the complete engine system is required. In Europe an engine like the ATE probably is not built by just one contractor; on the contrary, a number of subcontractors will, under the coordination and responsibility of a prime contractor, develop, build, and test the various components, which then will gradually be integrated into a complete engine.

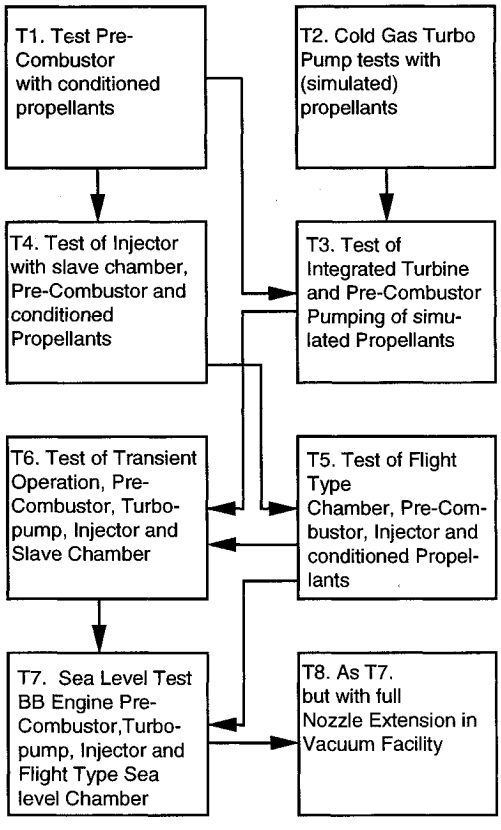

Fig. 11 Schematic of test philosophy for ATE.

A. Test Philosophy

Testing of individual components will be the responsibility of the subcontractor(s) for these components. The subcontractors may use dedicated test rigs of their own as long as this makes sense. For instance, a propellant pump may be tested with water and propellant in a dedicated test rig by a pump subcontractor. However, a complete turbopump, which has to be driven by a hot gas-generator, is easier developed and tested in conjunction with an engine gas-generator. It has, therefore, been decided to integrate the various components in as early a stage as possible. The sequence of the test philosophy is outlined in Fig. 11 for the breadboard phase. This clearly shows the gradual buildup of the test facilities for engine and component testing. Only the main development testing during the breadboard phase is shown. The development of smaller components like the valves and control system is not shown here, but proceeds in a similar way. Testing the various components this way minimizes the associated risks, the investment in test equipment, and development time.

B. Test Facilities

In Europe, various test facilities for component development are available. Both, Fiat Avio and Volvo Aero Corporation have facilities to develop and test turbopumps. Engine and component test facilities are available at DASA, DLR, and ESA in Lampoldshausen and at SEP. Royal Ordnance have test facilities for sea-level testing of components and the complete engine. Vacuum facilities, although available in Europe, will have to be modified to allow for this size of nozzle (area ratio 400) and to simulate TVC. All test facilities are computer controlled.

IX. Conclusions

Five major European propulsion companies have, under ESA contract, studied the feasibility of a 20-kN storable bipropellant pump-fed engine. This resulted in a versatile precombustion cycle engine design with a specific impulse exceeding 3440 m/s (350.6 s). The main components of this engine have been designed and analyzed in detail. Two options emerged: 1) a metallic engine with a mass of 74.2 kg and 2) an engine with a thrust chamber and nozzle extension made of ceramic composite material. The latter engine has a simplified cooling system and a mass of 57.9 kg.

Based on extensive development plans, it is estimated that the nominal development in Europe will take eight years and will cost 123 MAU. The recurrent cost for the ATE is estimated to be 1.68 MAU.

Because of its high performance, an ATE-like engine could substantially increase the capabilities of heavy launchers like Ariane 5 or Titan 4, especially if used in conjunction with an OPM. Using such an engine as an upper stage for Ariane 5 would increase the payload capability by 10%. The satellite lifetime or revenue earning payload also may be increased because of more payload into orbit. A typical large telecommunication satellite could increase its revenue earning capabilities by 60 MAU over eight years by increasing the number of transponders. By extending the amount of on-board propellant the satellite life may be extended by four to eight years, also resulting in a substantial increase of revenue earning potential.

Acknowledgments

The authors want to thank G. Andrei, G. Giordano, and A. Minervini from Fiat Avio; L. W. Hobbs and E. Kruzins from Matra Marconi Space; C. Etheridge, J. Harlow, A. Klepping, and A. J. Meade from Royal Ordnance; A. Mel-

chior, A. Louis, and A. Mathieu from SEP; T. Hannebäck and U. Palmnäs from Volvo Aero Corporation; and all their supporting staff for their excellent and enthusiastic execution of these studies. Also, the authors acknowledge the stimulating contribution from D. Hässler from DASA. Finally, the authors want to thank G. Saccoccia from ESTEC for his in-depth extension of the thermodynamic modeling of NTO.

References

[1]Smalley, M., "Advanced Technology Engine Mission Analysis, Volume 1, Earth Orbital Mission Analysis, Volume 1," British Aerospace, TN 5008, No. 1, Stevenage, Aug. 1987.

[2]Kruzins, E., "Orbital Propulsion Module System Engineering and Performance Comparison," British Aerospace, TNO/GP/50561, No. 1, Stevenage, Aug. 1991.

[3]Hobbs, L. W., "Utility Propulsion for the Space Station Era," AIAA Paper 89-2508, July 1989.

[4]Hobbs, L. W., "The Design of a General Purpose Modular Propellant Feed System," AIAA Paper 90-1939, July 1990.

[5]Elliott, C. A., "Advanced Technology Engine Mission Analysis, Volume 1, Earth Orbital Mission Analysis, Volume 2," British Aerospace, TP 8364, No. 2, Stevenage, July 1987.

[6]Klepping, A., and Horton, T., "Configuration and Mechanical Design Concept of the ATE," Royal Ordnance, A.T.E./SN/A5/1, Westcott, Oct. 1987.

[7]Andrei, G., "ATE Control Concept and Cycle Trade Off," Fiat Aviazione, TPP 87033, No. 2, Torino, Italy, March 1988.

[8]Palmnäs, U., "Engine System and Performance Analysis for High Pressure Gas Generator Cycle and Pre-Combustion Cycle Engines," Volvo Flygmotor AB, 336-90-R026, Trollhättan, March 1990.

[9]Kruzins, E., "Design Concept for a Staged Precombustor/Gas Generator," AIAA Paper 89-2841, July 1989.

[10]Dabinett, J., and Marsh, S., "Structural Evaluation Capability at Royal Ordnance with a Preliminary Analysis of the ATE Combustion Chamber," Royal Ordnance, SN Act. 7, Westcott, July 1991.

[11]Louis, A., "Assessment of the Use of SEP CMC Materials for the ATE Main Combustion Chamber and Nozzle Extension," SEP, TR/MC 2390/90CI LA/lc., Villaroche, June 1990.

[12]Louis, A., "Assessment of the Use of SEP Ceramic Matrix Materials for the Advanced Technology Engine," SEP, TR/MC 2444/90 LA/cm, Villaroche, Nov. 1990.

[13]Melchior, A., Pouliquen, M. F., and Soler, E., "Thermostructural Composite Materials for Liquid Propellant Rocket Engines," AIAA Paper 87-2119, June/July 1987.

[14]Wallin, S., "Combustion Chamber Cooling Analysis," Volvo, Rept. WP 6, Trollhättan, June 1990.

[15]Minervini, A., and Vinci, C., "Heat Transfer Calculations for a Regeneratively Cooled Rocket Engine," Fiat Aviazione, TPF 88088N, Torino, Italy, May 1988.

[16]Minervini, A., "Calculation of Coolant State for an Advanced Bi-Propellant Rocket Engine," Fiat Aviazione, TTPF87206, Torino, Italy, Dec. 1987.

[17]Saccoccia, G., "Extension of the NTO Computer Code for the Calculation of Thermodynamic and Transport Properties of Di-Nitrogen Tetroxide (N_2O_4) Under Critical Pressure," ESA/ESTEC, Noordwijk, The Netherlands, July 1991.

[18]Chilenski, J., and Lee, D. H., "An Experimental Investigation of the Performance of the Nitrogen-Tetroxide-Hydrazine System in the Oxidizer-Rich and Fuel-Rich Regions," Jet Propulsion Lab., NASA TR 32-212, March 1962.

[19]Bigert, M., and Wallin, S., "Performance Estimate and Preliminary Structural Design of Nozzle Extension," Volvo, SN WP-7, Trollhättan, March 1991.

[20]Rao, G. V. R., "Exhaust Nozzle Contour for Optimum Thrust," *Jet Propulsion*, Vol. 28, No. 6, 1958.

[21]Nickerson, G. R., Dang, L. D., and Coats, D. E., "TDK-Two Dimensional Kinetic Reference Computer Program," Software and Engineerng Associates, Inc., NASA-CR178628, 1985.

[22]Härefors, M., "Preliminary SC (and GG) Cycle Transient Model Analysis, and Comparison," Volvo, Rept. 314-5030/1, Trollhättan, Dec. 1990.

[23]Andrei, G., "Performance Optimization of a Staged Combustion Bi-Propellant Turbopump Feed System—Off Design Analysis," Fiat Aviazione, Torino, Italy, April 1988.

[24]Klepping, A., and Horton, T., "Determination of the Design Requirements," Royal Ordnance, A.T.E./SN/A4/1, Westcott, July 1987.

[25]Klepping, A., and Horton, T., "Thermodynamic Engine Cycle Analysis and Comparison for the ATE," Royal Ordnance, A.T.E./SN/A3/1, Westcott, May 1987.

[26]Etheridge, C. J., and Harlow, J., "CATE Upgrade and HPGG/PC Cycle Performance Analysis," Royal Ordnance, SN Act. 1, Westcott, Nov. 1990.